Section 3

Computational studies including new techniques, the effect of varying model resolution, parallel processing

Parallel version of the spectral model of the Hydrometcenter of Russia

Elena D. Astakhova and Yuri V. Alferov,
Hydrometeorological Research Center of the Russian Federation,
11-13, Bolshoi Predtechenskii per., 123242, Moscow, Russia,
e-mail: helen@mecom.ru, alferov@mecom.ru.

A parallel version of the spectral model of the Hydrometcenter of Russia [1, 2] was developed. It is based on the MPI technology and uses one-dimensional decompositions for computations in grid and spectral spaces. In the grid space, each processor element (PE) makes computations for two latitude belts located symmetrically with respect to the equator. The need for application of the two symmetric belts follows from symmetry of the Legendre polynomials. Because of this, the maximum number of PEs the model can run on is equal to the number of latitude rows divided by two. Another restriction on the number of PEs that can be used by the model follows from the decomposition of the spectral space in wavenumber, but it is less strong. The fast Fourier transformation programs used in the model were optimized for Intel compilers. The parallel versions of the T169L31 and T339L31 spectral model were tested on SMP computers based on Intel Itanium and Xeon processors. The results are demonstrated in Figs. 1 and 2. The additional application of SHMEM library for reduction operations was found to decrease communication costs and thus to improve the speedup (Figs. 1b and 2). The use of 'heavier' physics (compare variants with radiation block called at every time step and with cloud-radiation interaction computed once a day, Fig. 1(*a*)) makes the speedup better. This suggests that the future improvement of parameterizations of subgrid-scale processes, which will become more time-consuming, will not meet problems with computation time in multiprocessor mode. Note that the time necessary to integrate the T169L31 and T339L31 models on 32 PEs is small enough to use them in operational mode when a new computer arrives at the Hydrometcenter of Russia (in 2007). The development of the parallel version of the spectral model also makes it possible to use a model with higher resolution in the ensemble prediction system without decreasing the number of ensemble members.

It is expected that the parallel version of the T85L31 spectral model will be operationally used for deterministic medium-range forecasting at the Hydrometcenter of Russia after May 2006, while the T169L31 version is to be implemented in October 2006. The research ensemble prediction system will incorporate the parallel model in December 2005.

Acknowledgements

The authors are grateful to Intel Inc., Silicon Graphics Inc., and personally to V. Antsipovich, N. Mester, P. Shelepugin, I. Zakharov, and V. Tsvetkov for help and possibility to make computations.

The study was supported by the Russian Foundation for Basic Research (projects nos. 04-05-64530-a, 05-05-64575-a, and 04-07-90183-b).

References:

1. Kurbatkin, G.P., Astakhova E.D., Krupchatnikov, V.N., et al., 1987: A Medium-range Weather Prediction Model. *Doklady AN SSSR*, vol. 4, no.2
2. Frolov, A.V., Astakhova, E.D., Rozinkina, I.A., et al., 2004: On Practical Predictability of Meteorological Quantities by Global Spectral Model of the Hydrometcenter of Russia. *Russian Meteorology and Hydrology*, no. 5.

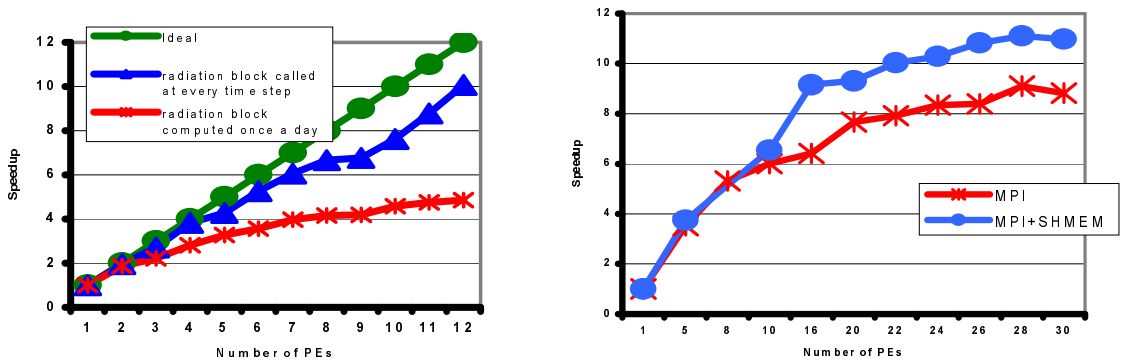

a) *b)*

Fig. 1. The speedup of the T169L31 (a) and T339L31 (b) models as a function of the number of processor elements.

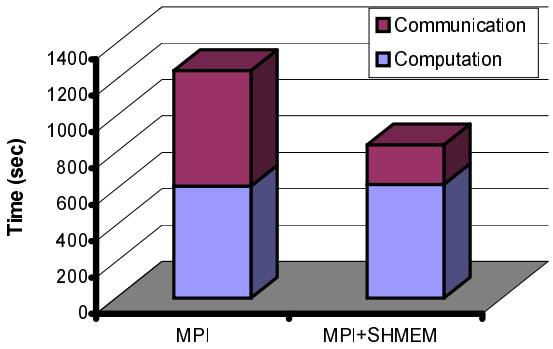

Fig. 2. Comparison of communication and computation costs for T339L31 based on MPI only and on MPI + SHMEM (32 PEs).

CLIMATE MODELING WITH SPECTRAL ELEMENTS

Ferdinand Baer, U. of Maryland, College Park, MD, baer@atmos.umd.edu. Houjun Wang, U. of Maryland; Joseph J. Tribbia, NCAR; Aimé Fournier, NCAR.

Our primary objective is to create accurate predictions of future climate on decadal to centennial time scales and on a broad spectrum of space scales by improving model-component performance and accuracy, by implementing efficient strategies to couple model components, and by maximizing throughput on state-of-the-art computers capable of exceptional peak speeds. To this end we have developed a climate model entitled Spectral Element Atmospheric Climate Model (CAM_SEM) that includes a unique dynamical core (SEAM) that is currently coupled to both the physics component of the Community Atmosphere Model (CAM) and its the land surface component (CLM). Our primary effort thereto has focused on the dynamical core (dycore) component. Included among the major improvements we hope to provide are a more transparent, efficient and accurate method of producing *regional climate predictions* involving local mesh refinement, improved numerical quadrature, a more comprehensive technique for predicting the overall global climate, and application of computing methodology using the latest in computing hardware most effectively and economically to produce the best predictions/simulations with minimal expenditure of resources.

One signature of climate change may be identified in the frequency and magnitude of deviations from the climate mean, and by the increased frequency of regional events such as hurricanes, or severe storm complexes that have significant impact on relatively short time and space scales. To uncover these phenomena model resolution must be increased, at least locally, with the consequence that processes effecting previously unresolved scales in coarser grained models must then be considered. Including shorter space scales introduces shorter time scales, thereby further increasing computational requirements. This highlights the importance of understanding the impact of the shorter space scales on predictions and how these scales interact with the larger scales in the coarse grained portion of the total domain, and also highlights the need to develop model methodology that optimizes the use of computer resources. Our methodology is formulated to take into account local scaling requirements, and dynamic scalability is achieved without distorting the overall global prediction. We utilize the advantageous features of computers for prediction on any and all space scales deemed significant, and do so in a seamless and rigorously convergent fashion.

Our modeling studies have exploited the spectral-element method. We developed a pioneering dycore for the global atmosphere, which we named the Spectral Element Atmosphere Model (SEAM), summarized in Fournier et al. (2004). Spectral elements have advantageous properties both for global modeling and for inclusion of regional space scales by using local mesh refinement (LMR), providing higher resolution in regions of strong local variability and generating regional predictions within a global model. The model is self-contained and is combined with appropriate physics and other scientific numerical *packages* as noted above.

Based on our runs with SEAM in the shallow water mode using the community test suite, we have established the model's flexibility, its ability to produce regional detail under LMR, its accuracy and computational efficiency when compared to similar models, and its advantages when using parallel processors. We subsequently ran SEAM under various representations as a

3D dycore and have found that in all circumstances it performed well, better or equivalently to competitive models. In this context, we studied the effects of varying resolution with and without the inclusion of the Earth's topography. Additionally, we made predictions with the SEAM dycore and simple Held-Suarez physics applying global and regional scaling concurrently, to check SEAM's skill using local mesh refinement (LMR), primarily over the continental United States. Results from these experiments indicate that LMR is working successfully in our dycore.

To generate a complete climate model, we coupled the state-of-the-art physics package algorithm developed for the CCSM system at NCAR (CAM), as well as the CLM (land model) algorithm to SEAM, creating CAM_SEM. A variety of experiments including the application of LMR were made to test this model. All experiments proved encouraging and culminated with an AMIP run for comparison with the variety of such experiments made available to PCMDI. We ran CAM_SEM with identical initial and boundary conditions to CAM2 (an NCAR submission to AMIP which included the same physics as we used) and we set our grid set as near as possible to T42. Our integration covered the period 1979 to 1998 for which input data were available. We compared CAM_SEM output to the output archives of CAM2 as well as NCAR archives that contain some observational data taken from reanalysis data over that period. The implications of these comparisons indicate that CAM_SEM is running in a stable mode and is producing results that look similar to those of CAM2. Since the integration period is 20 years, it is not possible to achieve identical results from different models, but the similarities noted are highly encouraging. These results have recently been submitted in a paper to Monthly Weather Review that is currently under review (Baer et. al, 2006).

Experiments with CAM_SEM are presently under development to include LMR as a contribution to the Stretched Grid Model Intercomparison Program (SGMIP).

References:

Baer, F., H. Wang, J. J. Tribbia, and A. Fournier, 2006: Climate modeling with spectral elements. *Mon. Wea. Rev.*, under review.

Fournier, Aimé, Mark A. Taylor and Joseph J. Tribbia, 2004: The Spectral Element Atmospheric Model: High-resolution parallel computation and response to regional forcing. *Mon. Wea. Rev.*, **132**, 726-748.

Decadal Climate Simulations with NCAR CAM Using Accurate and Fast Neural Network Emulation of Full, Long- and Short Wave, Model Radiation

Michael S. Fox-Rabinovitz[1], Phone: 301-405-5395, Fax: 301-405-8468, Email: foxrab@essic.umd.edu
Vladimir M. Krasnopolsky[1,2], Dmitry V. Chalikov[1], and Alexei Belochitski[1]
[1]Earth System Science Interdisciplinary Center, University of Maryland, USA
[2]SAIC at NCEP/NOAA

The approach to calculation of model physics using neural network (NN) emulations, previously proposed and developed by the authors, has been implemented for decadal climate model simulations. NN emulations of model physics are based on the fact that any parameterization of physics can be considered as a continuous or almost continuous mapping (input vector vs. output vector dependence), and NNs are a generic tool for approximation of such mappings [*Krasnopolsky et al. 2002*]. NN is an analytical approximation that uses a family of functions like:

$$y_q = a_{q0} + \sum_{j=1}^{k} a_{qj} \cdot \tanh(b_{j0} + \sum_{i=1}^{n} b_{ji} \cdot x_i); \quad q = 1, 2, \text{K}\ , m \tag{1}$$

where x_i and y_q are components of the input and output vectors respectively, a and b are fitting parameters, and hyperbolic tangent is a so called activation function, n and m are the numbers of inputs and outputs respectively, and k is the number of neurons in the hidden layer (for more details see appendix in [*Krasnopolsky et al., 2002*]).

The long-wave and short-wave radiation (LWR and SWR) parameterizations or the *full model radiation* [*J. of Clim. 1998 and the references to W. Collins therein*], the most time consuming component of model physics, have been emulated with neural networks (NN) for the NCAR CAM-2. The developed highly accurate NN emulations for LWR and SWR are two orders and one order of magnitude faster than the original/control NCAR CAM LWR and SWR, respectively [*Krasnopolsky et al. 2005, 2006*]. The NN emulations using 50 neurons in the hidden layer provide, if run *separately* at every model physics time step (1 hour), the speed-up of ~ 150 times for LWR and of ~ 20 times for SWR as compared with the original LWR and SWR, respectively. Using NN emulations *simultaneously* for LWR and SWR or for the full model radiation, results in a significant, ~ 13 times, acceleration of calculations of the entire/full model radiation block. It is worth clarifying that for the control run, the original LWR (including time consuming optical properties calculations) is calculated less frequently, only every 12 hours or twice a day, and only computationally inexpensive heating rates and radiative fluxes are calculated every hour. For the model run using NN emulations, LWR (including both optical properties and heating rates and radiative fluxes) is calculated more frequently, every hour, that is more consistent with SWR and other model physics calculations.

The results of decadal climate simulations performed with NN emulations for both LWR and SWR, i. e., for the full model radiation, have been validated against the parallel control NCAR CAM simulation using the original LWR and SWR. The almost identical results have been obtained for these parallel 40-year climate simulations (Fig. 1). (Note that the first 10 years of simulations are not included in validation to avoid the impact of spin-up effects, so that years 11-50 are used for validation.)

The temperature distributions for the parallel runs are close to each other and their deviation or mean bias is practically zero, with minimum and maximal biases within ~ 2-2.5 K

by magnitude, that is comparable with typical observation errors (as a reference). Close similarity has been also obtained for other model prognostic and diagnostic fields.

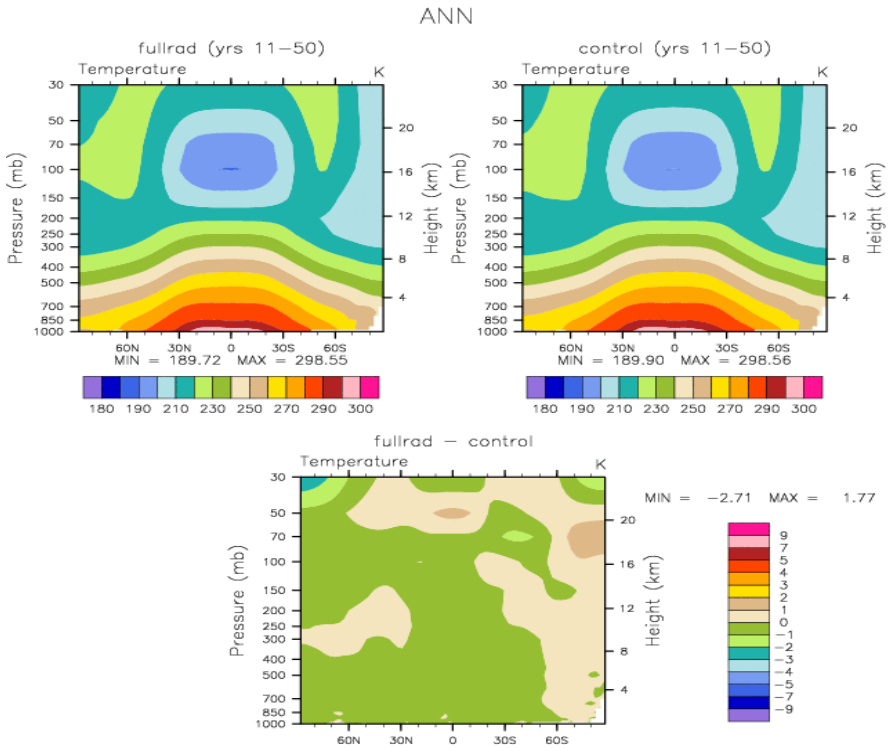

Fig. 1 Zonal mean vertical distribution of temperature, in K, for the 40-year period of NCAR CAM simulations with the NN emulations for the full model radiation (the upper left panel), the control (the upper right panel), and their difference or bias.

The obtained results open the opportunity of using efficient neural network emulations for full model radiation for decadal and longer climate simulations as well as for weather prediction models. The developed methodology can be applied to other LWR and SWR schemes used in the variety of models, process studies, and other applications.

Acknowledgments The authors would like to thank Drs. W. Collins, P. Rasch, and J. Tribbia (NCAR), for useful discussions and consultations.

References

Journal of Climate, 1998: v. 11, No. 6 (the special issue).

Krasnopolsky, V.M., M.S. Fox-Rabinovitz, and D.V. Chalikov, 2005: "Fast and Accurate Neural Network Approximation of Long Wave Radiation in a Climate Model", *Monthly Weather Review*, vol. 133, No. 5, pp. 1370-1383.

Krasnopolsky, V.M., and M.S. Fox-Rabinovitz, 2006: A New Synergetic Paradigm in Environmental Numerical Modeling: Hybrid Models Combining Deterministic and Machine Learning Components, *Ecological Modelling*, 191, pp. 5–18.

Krasnopolsky V. M., D. V. Chalikov, and H. L. Tolman, 2002: "A Neural Network Technique to Improve Computational Efficiency of Numerical Oceanic Models", *Ocean Modelling*, v.4, 363-383.

Regional Modeling with Variable-Resolution GCMs: Stretched-Grid Model Intercomparison Project (SGMIP)

Michael Fox-Rabinovitz, University of Maryland at College Park, U.S.A.,
Jean Côté and Bernard Dugas, Environment Canada, Canada,
Michel Déqué, Météo-France, France, and
John L. McGregor, CSIRO, Australia

Variable-resolution GCMs using a global stretched grid (SG) with enhanced resolution over the region(s) of interest have proven to be an established approach to regional climate modeling providing an efficient means for regional down-scaling to mesoscales. This approach has been used since the early-mid 90s by the French, U.S., Canadian, Australian and other climate modeling groups along with, or as an alternative to, the current widely-used nested-grid approach. Stretched-grid GCMs are used for continuous/autonomous climate simulations as usual GCMs, with the only difference that variable-resolution grids are used instead of more traditional uniform grids. The important advantages of variable-resolution SG-GCMs are that they do not require any lateral boundary conditions/forcing and are free of the associated undesirable computational problems. As a result, SG-GCMs provide self-consistent interactions between global and regional scales of motion and their associated phenomena, while a high quality of global circulation is preserved, as in uniform grid GCMs.

The international SGMIP-1 (Stretched-Grid Model Intercomparison Project, phase-1), using variable-resolution SG-GCMs developed at major centers/groups in Australia, Canada, France, and the U.S., has been successfully conducted in 2002-2005. The results of the 12-year (1987-1998) climate simulations for a major part of North America are available at the SGMIP web site: http://essic.umd.edu/~foxrab/sgmip.html, and are described by Fox-Rabinovitz et al. (2006). The climate simulation results obtained with the SGMIP-1 SG-GCMs have shown the maturity of the SG approach.

The multi-model SGMIP-1 regional climate simulations were conducted with enhanced 0.45° - 0.5° regional resolution for SG-GCMs, with the same or a similar number of global grid points as in a 1° x 1° global grid. The multi-year SGMIP-1 SG-GCM simulations were analyzed in terms of studying the impact of high regional resolution on efficient downscaling to realistic mesoscales and regional climate variability. We focused mostly on studying the quality of the multi-model ensemble results. The differences between the models have been also determined. The SGMIP-1 multi-model ensemble results for the region compare well with reanalysis and observations, in terms of spatial and temporal diagnostics.

This is what has been learned from SGMIP-1:

(a) the appropriate *moderate stretching* design for long-term climate simulations has been defined;

(b) the SG-approach works well and is *robust* for SG-GCMs with *different dynamics and physics*; namely, for dynamics using spectral and grid-point schemes, with spherical and geodesic grids, and for physics calculated at intermediate uniform or variable resolution for the resolution range of 0.5º to 2º- 4º (with a moderate stretching);

(c) the SGMIP-1 SG-GCMs provide *high quality regional and global* climate simulation products, with differences between the models documented by producing the Taylor diagrams;

(d) the *advantage of using the multi-model ensemble* mode has been demonstrated, in the sense that the multi-model ensemble means are closer to reanalyses and observations than the individual ensemble members;

(e) improvements associated with better resolved land-sea differences may be obtained when using larger ensembles, (see also e.g. Fox-Rabinovitz et al. 2005).
Other major SGMIP-1 results are as follows:
1. Efficient regional *downscaling to realistic mesoscales* is obtained with small/limited regional biases, for time averaged model products, that are a fraction (~50% or less) of reanalysis or observational errors. Biases are larger, up to twice the reanalysis or observational errors (but only for the southern polar domain); note that our SGs have the North American area of interest. *Overall, biases are within the uncertainties of available reanalyses.*
2. Both seasonal and interannual *climate variability* are *well represented*. Namely, annual cycles, seasonal differences, time series, and variances are close to those of observations or reanalyses.
3. Orographically induced precipitation and other products are well simulated at meso- and larger scales due to high-resolution regional forcing. The *major positive* regional impact *from stretching* is directly obtained from *better resolved* model dynamics and regional *enhanced resolution stationary boundary forcing*, i.e. orography and land-sea differences. In that sense, the improvements are obtained near small-scale terrain features and coastlines, and are reflected, for example, in the Appalachian and coastal precipitation.
The future SGMIP plans, SGMIP-2 (phase-2), include comparisons of high resolution stretched and uniform grid GCMs, with the prime area of interest over the major part of North America. These SGMIP-2 experiments will provide the possibility for a *comprehensive analysis of enhanced variable and uniform resolution GCMs* and their *high resolution multi-model ensembles* against reanalysis and observations. The SGMIP-2 experiments will be conducted for the 25-year period of integration, from 1979 to 2003. SGMIP-1 and SGMIP-2 have been endorsed by the WMO/WGNE at its 2004 annual meeting and the progress report has been presented at its 2005 annual meeting. The SGMIP products are available to national and international programs such as WMO/ WCRP/WGNE, CLIVAR, GEWEX, IPCC. The SGMIP effort, aimed at introduction of the SG-GCMs to a broader regional and global climate modeling community, contributes to a better understanding of the efficient SG-approach to climate modeling and the variety of applications.

References

Fox-Rabinovitz, M. S., E. H. Berbery, L.L. Takacs, and R.C. Govindaraju, 2005: A multiyear ensemble simulation of the U.S. climate with a stretched-grid general circulation model", *Mon. Wea. Rev.,* 133, pp. 2505-2525.
Fox-Rabinovitz, M.S., J. Cote, M. Deque, B. Dugas, J. McGregor, 2006: Variable-Resolution GCMs: Stretched-Grid Model Intercomparison Project (SGMIP), *J. Geophys. Res.*, in press.

The ICON dynamical core project: modelling strategies and preliminary results

Marco Giorgetta, Luis Kornblueh, Erich Roeckner, Hui Wan
Max Planck Institut für Meteorologie
Bundesstr. 53, 20146, Hamburg, Germany
e-mail: giorgetta@dkrz.de, kornblueh@dkrz.de, roeckner@dkrz.de, wan@dkrz.de

Thomas Heinze, Detlev Majewski, Pilar Rípodas
Deutscher Wetterdienst
Kaiserleistr. 42, 63067, Offenbach, Germany
e-mail: thomas.heinze@dwd.de, detlev.majewski@dwd.de, maria-pilar.ripodas@dwd.de

Luca Bonaventura
MOX - Politecnico di Milano
P.zza Leonardo da Vinci 32, 20133, Milano, Italy
e-mail: luca.bonaventura@polimi.it

The ICON project is a joint development effort of MPI-M and DWD to achieve a unified climate and NWP model using geodesic grids with local grid refinement. The model under development in the ICON project will use the fully elastic, nonhydrostatic Navier-Stokes equations, which provide a framework that is sufficiently general for meteorological applications on most scales relevant to numerical weather prediction and climate simulation.

As an intermediate step, a semi-implicit discretization for the hydrostatic primitive equations is being developed. The proposed horizontal discretization uses the triangular Delaunay cells of the icosahedral grid as control volumes. It achieves mass and potential enstrophy conservation, thus replicating the results of [4] for standard rectangular C grids. Vector radial basis function interpolation is used to reconstruct a uniquely defined velocity field from the velocity components normal to the cell sides, which are the discrete model variables along with the cell averaged values of the mass variables like pressure, temperature or geopotential height. A full description of the horizontal discretization can be found in [1], [2]. One result obtained with a preliminary shallow water implementation on an idealized test case (see [5]) is shown in figure 1(a). The difference in the geopotential height field after 15 days of simulation between the model using 327680 triangles (approximately 40 km horizontal resolution) and a reference field obtained with resolution T426 of a slightly modified NCAR spectral shallow water model [3] are presented. Application of the same technique to a hydrostatic model with local grid refinement option is currently being investigated. Figure 1(b) and (c) show two possible computational grids, with different local refinement strategies.

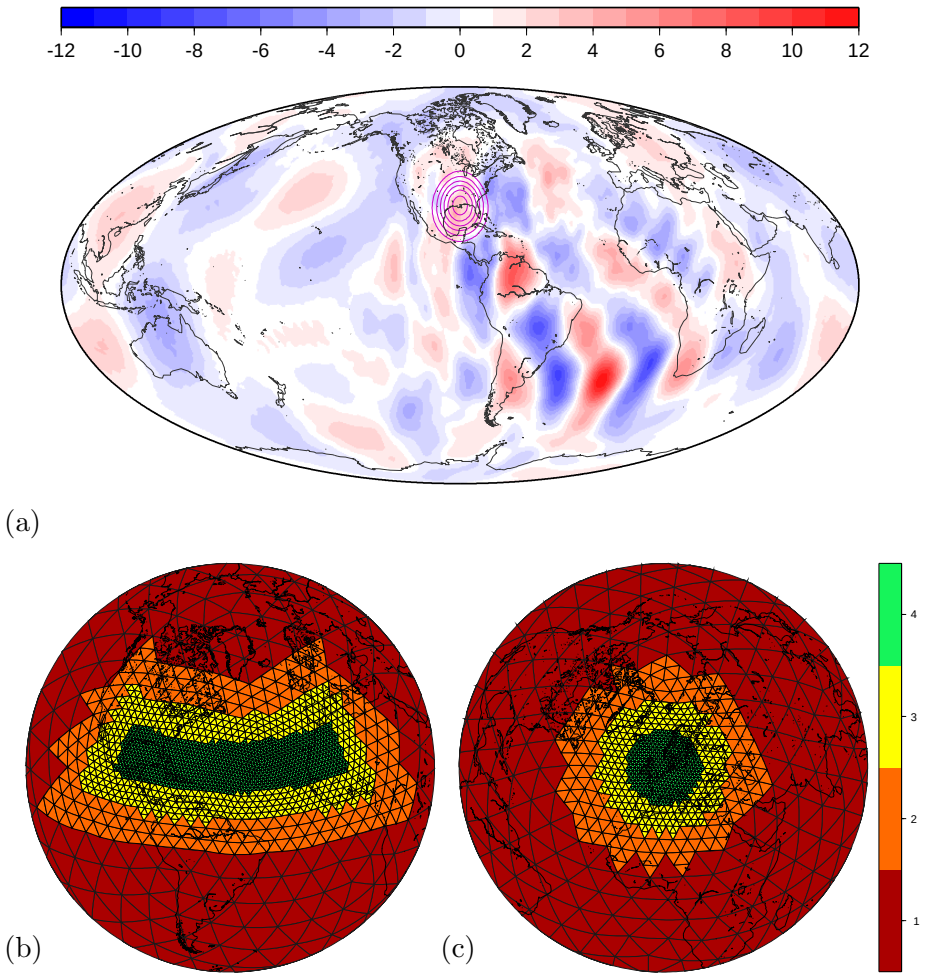

Figure 1: (a) Difference to reference of geopotential height field after 15 days for test case 5 of [5]. Reference is modified NCAR spectral shallow water model with resolution T426 [3]. (b) and (c) Two configurations of the computational grid with local refinement option using 4 refinement steps.

References

[1] L. Bonaventura, L. Kornblueh, Th. Heinze, and P. Rípodas. A semi-implicit method conserving mass and potential vorticity for the shallow water equations on the sphere. *International Journal of Numerical Methods in Fluids*, 47:863–869, 2005.

[2] L. Bonaventura and T. Ringler. Analysis of discrete shallow water models on geodesic Delaunay grids with C-type staggering. *Monthly Weather Review*, 133:2351–2373, 2005.

[3] P. Rípodas, L. Bonaventura, and L. Kornblueh. New reference solutions for the Williamson et al. (1992) shallow water test cases. Online available at `http://icon.enes.org`, 2005.

[4] R. Sadourny. The dynamics of finite difference models of the shallow water equations. *Journal of the Atmospheric Sciences*, 32:680–689, 1975.

[5] D.L. Williamson, J.B. Drake, J.J. Hack, R. Jakob, and R.N. Swarztrauber. A standard test set for numerical approximations to the shallow water equations in spherical geometry. *Journal of Computational Physics*, 102:221–224, 1992.

Analysis of the Generalized Vertical Coordinate for the Euler Equations of Atmospheric Motion

Ilian Gospodinov[1]
National Institute of Meteorology and Hydrology, Bulgaria

It has been known that for the successful modeling of mesoscale atmospheric events with an essentially vertical structure of motion it is natural to use the full non-hydrostatic system of Euler equations rather than their hydrostatic approximation. It has also been known that the hydrostatic approximation can be constructed with the hydrostatic pressure as a vertical coordinate. Kasahara (1974) tried to summarize the transformation of the vertical coordinate for the governing equations of atmospheric motion. However, he did not discuss the transformation of the vertical momentum equation. Laprise (1992) proposed a form of the full system of non-hydrostatic equations with pseudo-hydrostatic pressure as a vertical coordinate. He affirmed that such approach is consistent and without loss of generality. This approach has been chosen by Bubnova et al. (1995) to build a new non-hydrostatic dynamical kernel of the ALADIN NWP limited-area model. However, the non-hydrostatic ALADIN remained in research mode until the beginning of the 21st century. The research on the non-hydrostatics benefited from the parallel work on the semi-Lagrangian technique of advection which brought into evidence some important issues such as the construction and the use of the vertical acceleration in a hydrostatic model (e.g.: Gospodinov et al. 2002). Benard et al. (2004) advanced significantly in the development of the non-hydrostatic ALADIN based on the Laprise's system.

In this work we attempt to go further than Kasahara (1974) and write the full non-hydrostatic system of Euler equations with generalized vertical coordinate. We attempt to derive the system of Laprise (1992) with pseudo-hydrostatic pressure as a vertical coordinate within the considerations of our theory. We analyze the properties of the system of Laprise (1992) by developing a split system. We attempt to situate the vertical acceleration in the full transformed system and in the system of Laprise (1992). The results of this study suggest that the system of Laprise (1992) is restricted with regards to the full non-hydrostatic system. It is possible to derive a measure of the error, introduced into the system with the particular choice of a vertical coordinate, namely the pseudo-hydrostatic-pressure vertical coordinate. The measure of error for the evolution tendency for the vertical derivative

[1]Email: ilian.gospodinov@meteo.bg

of the advecting vertical velocity is given by the following expression:

$$\left(\left(\frac{\partial \mathbf{V}}{\partial x}\right)_{\pi} \cdot \nabla_{\pi}\right)\mathbf{V} + \left(\left(\frac{\partial \mathbf{V}}{\partial y}\right)_{\pi} \cdot \nabla_{\pi}\right)\mathbf{V} + \frac{\partial \mathbf{V}}{\partial \pi} \cdot \nabla_{\pi}\dot{\pi} \ ,$$

where the notation is as in Laprise (1992). By analyzing the split model, it is also possible to be shown that the physical vertical velocity, within the system of Laprise (1992), is a diagnostic value and not a fully independent variable. If we want to build a non-hydrostatic model with a specific vertical coordinate, different from the geometric height, it is essential to define the law of evolution for the advecting vertical velocity which should not be a diagnostic relation of the type of the pseudo-hydrostatic-pressure coordinate of Laprise (1992).

References:

Benard, P., R. Laprise, J. Vivoda, and P. Smolikova, 2004: Stability of Leapfrog Constant-Coefficients Semi-Implicit Schemes for the Fully Elastic System of Euler Equations: Flat-Terrain Case. *Mon. Wea. Rev.*, **132,** 1306-1318.

Bubnova, R., G. Hello, P. Benard, and J.-F. Geleyn, 1995: Integration of the fully elastic equations cast in the hydrostatic pressure terrain-following coordinate in the framework of the ARPEGE/Aladin NWP system. *Mon. Wea. Rev.*, **123,** 515–535.

Gospodinov, I., V. Spiridonov, P. Benard, and J.-F. Geleyn, 2002: A refined semi-Lagrangian vertical trajectory scheme applied to a hydrostatic atmospheric model. *Q. J. Roy. Meteor. Soc.*, **128,** 323–336.

Kasahara, A., 1974: Various vertical coordinate systems used for numerical weather prediction. *Mon. Wea. Rev.*, **102,** 509–522. [See also Corrigendum: *Mon. Wea. Rev.*, **103,** 664.]

Laprise, R., 1992: The Euler equations of motion with hydrostatic pressure as an independent variable. *Mon. Wea. Rev.*, **120,** 197–207.

MPH: a Library for Coupling Multi-Component Climate Models and its Applications

Yun He and Chris H.Q. Ding, Computational Research Division, Lawrence Berkeley National Laboratory, Berkeley, CA 94720. yhe@lbl.gov, chqding@lbl.gov

A growing trend in developing large and complex applications on today's Teraflop scale computers is to integrate stand-alone and/or semi-independent program components developed by different institutions into a comprehensive simulation package. One example is the Community Climate System Model, which consists of atmosphere, ocean, land-surface and sea-ice components.

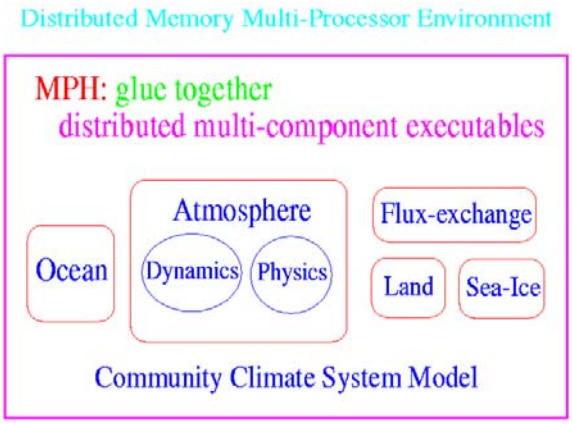

In CCSM, each component model is compiled into a binary executable image, like a standalone program. When CCSM is launched on a distributed memory computer, these component models are loaded into different set of processors; however, each model does not know the other models, their names, their processor-allocations, etc. A critical task on such distributed memory multi-component computer is a handshaking process that enables every component models to get the necessary information about other component models.

We develop a general-purpose multi-program handshaking (MPH) library to setup the distributed multi-component environment: for different executables to recognize each other, for setting up a registry of executable names and communication channels among different components. MPH must meet the following requirements: (a) Flexible component names. As CCSM is developed, component model and their names evolve. For example, atmosphere model changes from CCM to CAM, land-surface model changes from LSM to CLM, etc. Thus component names cannot be hardwired into the coupler. (b) Allow several model integration mechanisms. In CCSM 1, each component model is a single executable. In the related PCM (parallel climate model), each component model is a subroutine, and all component models are compiled into a single executable. As CCSM evolves, a component model could have several sub-components. Final ensemble simulations requires yet another multi-instance mechanism. (c) Resource allocation. Processor allocation must be flexible and only need to be specified at runtime through a simple controlling mechanism. All these requirements are met by MPH. In addition, a number of further utilities are provided as well.

For the first time, we clearly identify five effective execution modes and develop the MPH library to support application developments for utilizing these modes.

(1) Single-Component Executable, Single-Executable application (SCSE)
(2) Single-Component Executable, Multi-Executable application (SCME) **CCSM mode**
(3) Multi-Component Executable, Single-Executable application (MCSE) **PCM mode**
(4) Multi-Component Executable, Multi-Executable application (MCME) **most flexible mode**
(5) Multi-Instance Executable, Multi-Executable application (MIME) **ensemble simulations**

MPH provides the key infrastructure for integrating separate executables together. It provides functionalities for component name registration, resource allocation and initialize communication channels between independent components. MPH also supports components-joining, inter-component communication, inquiry on multi-component environment, and redirect input/output. MPH provides a flexible, versatile mechanism for these tasks, which are foundations for larger software tools/frameworks.

MPH provides a convenient framework to do the ensemble simulations. A multi-instance executable is a special type of executable. It differs from regular single-component and multi-component executables in that this particular executable is replicated multiple times (multiple instances) on different processor subsets. This enables running ensembles simultaneously as a single job, and ensemble averaging being done on the fly. Not only is this an effective way of using existing computing resources, it also reduces the potential human error by reducing the number of jobs that need to monitored. This eliminates large data output and storage for post-processing averaging, and enables on-the-fly nonlinear ensemble statistics that are otherwise impossible to compute as a post-processing step.

All MPH functionalities are currently working on IBM SP, SGI Origin, HP AlphaServer SC, and Linux clusters. MPH has been adopted in CCSM development, which is the U.S. flagship coupled climate model system heavily used in long-term climate research and government policy matters. A Model Coupling Toolkit for communication between different component models uses MPH. MPH has also been adopted in NCAR's Weather Research and Forecast (WRF) model and the Colorado State University's geodesic grid coupled model. Edinburgh Parallel Computing Centre (EPCC) uses MPH for ensemble simulations. Many other users for multi-instance simulations include MM5, WRF, ECMWF, Ocean DieCAST model, and a Monte Carlo code running on 1024 processors.

One of the applications for MPH is the concurrent single-executable development of CCSM. A multi-executable code integrates these components together as a single computational system while keep each component as a standalone executable. CCSM is currently such a multi-executable system based on the MPMD mechanism. It is cumbersome in usage and not available for machines without MPMD. So, single-executable CCSM is under request. We are developing a concurrent single-executable version of CCSM that coexists with multi-executable option. It is accomplished by redesigning the top level CCSM structures using MPH. We also proposed a module-based approach to solve name conflict issues associated with single-executable CCSM.

Both MPH multi-instances and single-executable development work improve future HEC capability for realizing next generation climate models. Detailed information is at: http://hpcrd.lbl.gov/SCG/acpi/MPH/ and http://hpcrd.lbl.gov/SCG/acpi/SE.

Acknowledgement: MPH is developed in collaboration with Tony Craig, Brian Kauffman, Vince Wayland and Tom Bettge of National Center of Atmospheric Research, and Rob Jacobs and Jay Larson of Argonne National Laboratory. This work is supported by a DOE SciDAC Climate Project and NERSC Program.

References:

Y. He and C. Ding, Coupling Multi-Component Models with MPH on Distributed Memory Computer Architectures, *International Journal of High Performance Computing Applications*, Vol.19, No.3, 329-340, August 2005. Earlier versions in *Proceedings of International Parallel and Distributed Processing Symposium*, April 2004, and *Proceedings of Realizing Teracomputing, the Tenth ECMWF Workshop on the Use of High Performance Computing in Meteorology,* November 2002.

Ensemble of Neural Network Emulations for Model Physics: The Impact on Climate Simulation

Vladimir M. Krasnopolsky[1,2], Phone: 301-763-8000 x 7262, Fax: 301-763-8545,
Email: Vladimir.Krasnopolsky@noaa.gov
Michael S. Fox-Rabinovitz[1], and A. Belochitski[1]
[1]Earth System Science Interdisciplinary Center, University of Maryland, USA
[2]SAIC at NCEP/NOAA, USA

1. Introduction

In our previous studies, we developed NN emulations of climate model physics for the NCAR CAM-2 [1, 2]. Specifically, a number of the NN emulations of the original long wave radiation (LWR) have been individually trained, with slightly different approximation and interpolation accuracies. In this study, we investigate the ability of NN ensembles, created from these NN emulations, to provide a better approximation and interpolation than their individual ensemble members, and to assess the NN ensemble impact on climate simulation.

As a nonlinear model or nonlinear approximation, the NN approximation problem allows for multiple solutions or for multiple NN emulations of the same LWR. For example, the original LWR, used in NCAR CAM, can be approximated with NNs with different numbers of hidden neurons, with different weights (resulting from the NN training with different initializations), different partitions of the training set, etc. The availability of multiple NN emulations, providing complimentary information about the original parameterization, opens an attractive opportunity of introducing a NN ensemble approach. It allows for integrating the complimentary information, contained in the individual ensemble members, into an ensemble that "knows" more about or represents the original LWR better than each of the individual ensemble members (a particular NN emulation). Moreover, the NN ensemble, when it is used in a climate model instead of a single NN emulation of the original LWR, may provide a better accuracy of the climate simulation.

An ensemble of NNs consists of a set of members, which are individually trained NNs. Their outputs are combined when applied to a new input data to improve the interpolation ability. We used a conservative ensemble [3] with a simple (with equal weights for all members) averaging of the member outputs providing the ensemble statistics.

2. NN ensemble for NCAR CAM LWR

The NN ensemble approach is an extension of our development of NN emulations we worked on for the last several years. Our approach to developing NN emulations for NCAR CAM LWR is described in detail in [1]. NCAR CAM-2 is integrated for two years to generate representative data sets for training, validation and test of NN emulations. All NN emulations and ensembles of the NN emulations are tested against the control which within our framework is obviously the original NCAR CAM LWR. Mean difference B (bias, or a systematic error) and the standard deviation (SD) of the difference between the original LWR and its NN emulation (random error), maximum and minimum errors, are calculated.

The final and the most important test is performed by estimating the accuracy of decadal climate simulation runs with single NN ensemble members and with the NN ensemble vs. the control climate run with the original NCAR CAM LWR. We have selected a sufficiently diverse

group of six NN emulations from the NN emulations we have already trained. Four of six members have the same architecture and were trained with perturbed initial conditions for the NN weights. Two others have different number of hidden neurons. These six NN emulations constitute the NN ensemble. Climate simulations have been run with NCAR CAM for 25 years with each of these six ensemble members (each of the six LWR NN emulations). The results

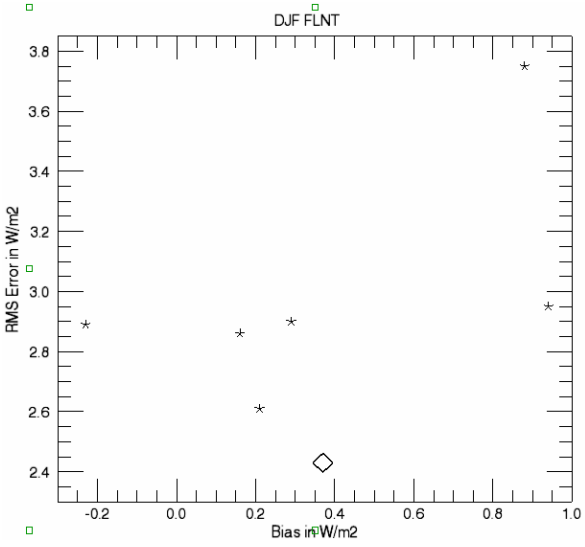

(climate fields and diagnostics) of each simulation are compared with the control climate run of NCAR CAM performed with the original LWR. The climate simulation errors (systematic, random, maximum, and minimum) have been calculated for each ensemble member. For the net LWR flux at the top of the model atmosphere (FLNT or OLR in W/m², for DJF (Dec-Jan-Feb)), bias and RMS errors for each ensemble member are shown as stars in the figure on the left. Then the NN ensemble climate run has been performed. For this run, six NN emulations are applied and the LWR outputs are calculated as the mean of these six NN emulation outputs, at each time step and at each grid point throughout the model integration. The use of the NN ensemble in climate simulation significantly reduces the systematic error (bias); it also reduces the RMS error to the value smaller than that of the best individual ensemble member. Bias and RMS error for the ensemble are shown as diamond in the figure. A significant reduction is obtained for the extreme errors as well.

3. Conclusions

A new NN ensemble approach is presented. It is applied to NN emulations of the LWR parameterization in NCAR CAM-2. It is shown that practically all individual NN emulations of LWR that we have trained in the process of developing an optimal NN LWR emulation, can be used within the NN ensemble approach for climate simulation. Using the NN ensemble results in a significant reduction of climate simulation errors, namely the systematic and random errors, the magnitudes of the extreme errors or outliers and, in general, the number of large errors.

References

[1] V.M. Krasnopolsky, M.S. Fox-Rabinovitz, and D.V. Chalikov, "New Approach to Calculation of Atmospheric Model Physics: Accurate and Fast Neural Network Emulation of Long Wave Radiation in a Climate Model", *Monthly Weather Review*, v. 133, No. 5, pp. 1370-1383, 2005.

[2] V.M. Krasnopolsky and M.S. Fox-Rabinovitz , "A New Synergetic Paradigm in Environmental Numerical Modeling: Hybrid Models Combining Deterministic and Machine Learning Components", *Ecological Modelling*, v. 191, pp. 5-18, 2006.

[3] S.V. Barai and Y. Reich, “Ensemble modeling or selecting the best model: Many could be better than one”, *Artificial Intelligence for Engineering Design, Analysis and Manufacturing*, 13, pp. 377-386, 1999

Parallel Calculations of Dynamics and Physics Blocks in Atmospheric General Circulation Model

V.P. Parkhomenko

Computing Centre of the Russia Academy of Sciences

Vavilov Str. 40 Moscow 119967 Russian Federation

E-mail: parhom@ccas.ru

The purpose of the work is to analyze components of AGCM algorithm and their parallel performance depending on computing efficiency of the program, to find bottlenecks which interfere with efficiency of parallel algorithm and to use the best procedures and more effective parallel strategy of performance, to increase speed of AGCM running on parallel systems.

A two-dimensional grid partition in the horizontal plane is used in the parallel implementation of the AGCM model. In this case there are basically two types of processor data exchanges. Data exchanges are necessary between logically coupled processors at calculations of finite differences; the removed data exchanges are necessary to carry out operations of spectral filtering, in particular.

The offered parallelization method assumes simultaneous calculation of the contribution of physics and dynamics blocks of model equations accordingly on two groups of processors from the same input data. Method realization demands change of the numerical scheme of time integration. The original scalar program was modified according to the reasons stated above. Model calculations were carried out up to steady state on the original and modified variants of the program for check of method correctness. They began from identical initial conditions.

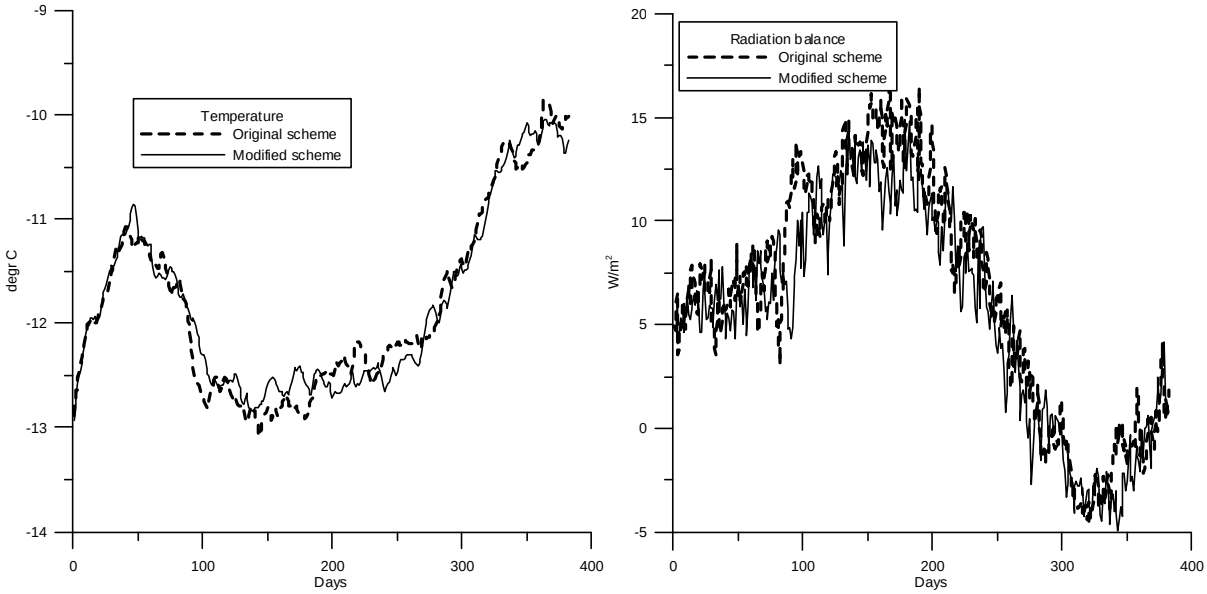

Fig. 1. Dependences of mean global temperature (at the left) and radiation balance (on the right) on the top border of an atmosphere from time for the original and modified schemes

The general feature of distributions of the basic climatic characteristics designed under initial and modified time integration scheme - the peak differences of results are observed in high latitudes in the winter season. It is connected, apparently, with snow distribution changes, and intensive non-stationary convective processes in an atmosphere. Ground

temperatures differences in more than 90 % of cells are less then 2°Ñ. Only in two cells in the winter in Northern hemisphere above the continents the difference is 10° Ñ. For winter season in the Southern hemisphere the similar picture is observed: appreciable differences exist in three cells in Antarctica. Sea level pressure differences do not exceed 15 mb in several cells and basically make less than 5 mb.

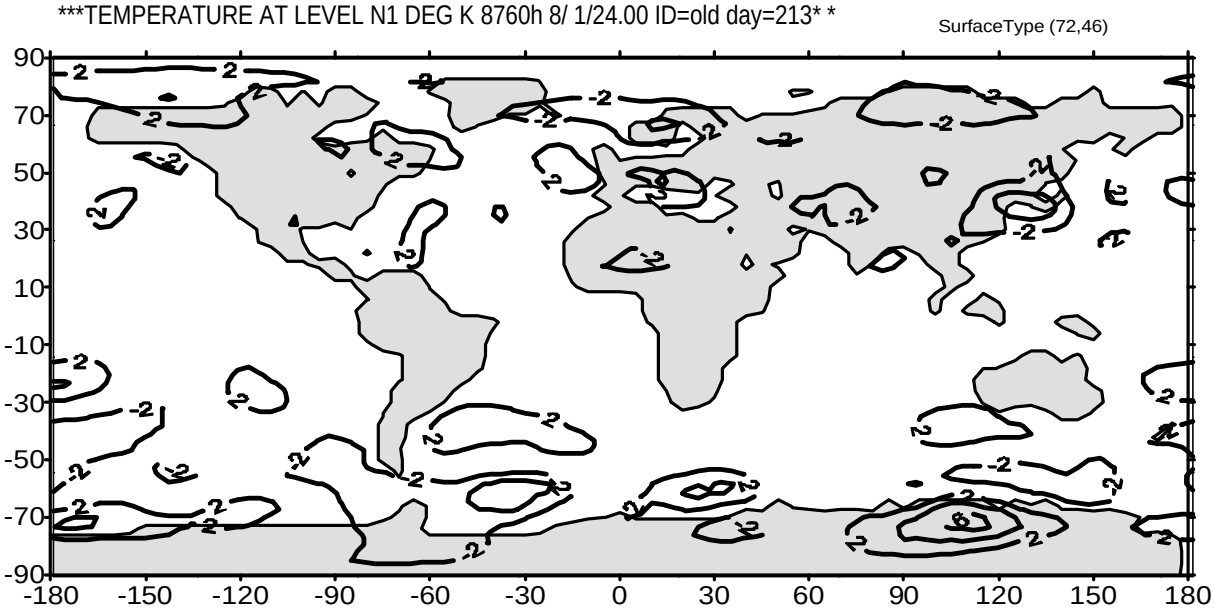

Fig. 2. July air temperature differences at 400 mb level for original and modified schemes.

At a level 400 mb air temperature differences do not exceed everywhere 2° Ñ, except for one point where achieve 6° Ñ. At a level 800 mb a picture is similar. It is possible to assert, that differences in results are more essential in surface areas.

Realization of the parallel program for various ways of splitting of global area on processors in climatic model is carried out. Updating of the time integration numerical scheme for an opportunity of realization of parallel calculations of dynamics and physics blocks with an estimation of computation efficiency is carried out. The analysis shows, that results of calculations under the modified scheme yields satisfactory results and its application is possible. In the scalar program physics block run time takes 38%, and dynamics block run time - 62%. It means that parallel program acceleration in one and a half time can be achieved. Offered procedure is used together with parallel computations of dynamics and physics blocks on the basis of global area decomposition. It allows to optimize loading of processors and to increase program efficiency. Results of application of loading balance of the physics block of AGCM enable additional reduction of running time on 15-20 %. Other opportunity of method application is a complication of the physics block without increasing of total computational time.

References

A. Arakawa and V. Lamb, "Computational Design of the Basic Dynamical Processes of the UCLA General Circulation Model.", Methods in Comp. Phys. 17 (1977) 173-265.

Lou, J. Z., J. D. Farrara, Performance Analysis and Optimization on a Parallel Atmospheric General Circulation Model Code, ISSN 1063-7133/97, 1997.

V.P. Parkhomenko Parallel Atmospheric General Circulation Model Code Analysis and Optimization. Research activities in atmospheric and oceanic modelling. World Meteorological Organization Geneva Switzerland 2005, V. 35, p. 3.19 – 3.20.

FINITE VOLUME SOLUTION OF THE SHALLOW WATER EQUATIONS ON THE SPHERE

Janusz A. Pudykiewicz, Environment Canada, RPN, e-mail: Janusz.Pudykiewicz@ec.gc.ca

The finite volume discretization developed for the numerical approximation of the scalar conservation laws on a geodesic mesh described in [1] was extended to the shallow water equations on the sphere:

$$\frac{\partial \mathbf{v}}{\partial t} + (\zeta + f)(\mathbf{k} \times \mathbf{v}) = -\nabla\big(gh + \frac{\mathbf{v}\mathbf{v}}{2}\big), \quad \frac{\partial h^\star}{\partial t} + \nabla(h^\star \mathbf{v}) = 0, \tag{1}$$

where $\mathbf{v}$ is the velocity field on the sphere, ζ is the vertical component of the vorticity, f is the Coriolis parameter, $h^\star$ is the geopotential height, h_s is the surface height, $h = h_s + h^\star$, $\mathbf{k}$ is the unit vector normal to the sphere, and g is the gravity acceleration.

The system of equations (1) is discretized on a geodesic icosahedral grid composed of triangles with vertices located on the spherical surface (Fig. 1). The control volume, Ω_i, associated with the i^{th} node is created by a two step procedure. In the first step, the centers of the triangles and the mid-points of the edges are projected on the surface of the sphere. In the second step, Ω_i is defined as a polygon with the vertices located at the projected points (Fig. 2). The semidiscrete version of (1) can be written compactly in the following form:

$$\frac{d}{dt}\begin{pmatrix} \mathbf{u}_x \\ \mathbf{u}_y \\ \mathbf{u}_z \\ \mathbf{h}^\star \end{pmatrix} = \begin{pmatrix} -\mathbf{G}_x(g(\mathbf{h}^\star + \mathbf{h}_s) + \mathbf{U}) - \mathbf{W}_x + \nu\mathbf{D}^4\mathbf{u}_x \\ -\mathbf{G}_y(g(\mathbf{h}^\star + \mathbf{h}_s) + \mathbf{U}) - \mathbf{W}_y + \nu\mathbf{D}^4\mathbf{u}_y \\ -\mathbf{G}_z(g(\mathbf{h}^\star + \mathbf{h}_s) + \mathbf{U}) - \mathbf{W}_z + \nu\mathbf{D}^4\mathbf{u}_z \\ -\mathbf{D}_x(\mathbf{h}^\star\mathbf{u}_x) - \mathbf{D}_y(\mathbf{h}^\star\mathbf{u}_y) - \mathbf{D}_z(\mathbf{h}^\star\mathbf{u}_z) \end{pmatrix}, \tag{2}$$

where $\mathbf{u}_\eta$, $\mathbf{h}^\star$ are the vectors of the control volume average values of the velocity components and the geopotential height respectively ($\mathbf{u}_\eta = \{v_{\eta\,1}, \ldots, v_{\eta\,N}\}$, N is the number of control volumes), $\mathbf{W}_\eta = (\zeta + f)(\mathbf{k} \times \mathbf{v})_\eta$, $(\eta \equiv x, y, z)$, $\boldsymbol{\zeta} = \mathbf{Z}_x\mathbf{u}_x + \mathbf{Z}_y\mathbf{u}_y + \mathbf{Z}_y\mathbf{u}_y + \mathbf{f}_c$, $\mathbf{U}$ is the vector of grid cell averages of $v^2/2$, and ν is the hyperviscosity coefficient. The operators in (2) are defined by the following relations:

$$(\mathbf{D}_\eta\boldsymbol{\psi})_i = \sum_{j(i)}\left(\frac{1}{2}(\psi_i + \psi_{j(i)}) + \frac{L_{ij(i)}}{8}\big(\mathbf{h}^a_{ij(i)}\nabla_0^{(0.25,0.75)}\psi\big|_i - \mathbf{h}^b_{ij(i)}\nabla_0^{(0.25,0.75)}\psi\big|_{j(i)}\big)\right)\gamma^\eta_{ij(i)} \tag{3}$$

$$(\mathbf{G}_\eta\boldsymbol{\psi})_i = \sum_{j(i)}\left(\frac{1}{2}(\psi_i - \psi_{j(i)}) + \frac{L_{ij(i)}}{8}\big(\mathbf{h}^a_{ij(i)}\nabla_0^{(-0.75,0.75)}\psi\big|_i - \mathbf{h}^b_{ij(i)}\nabla_0^{(-0.75,0.75)}\psi\big|_{j(i)}\big)\right)\gamma^\eta_{ij(i)} \tag{4}$$

$$(\mathbf{Z}_\eta\boldsymbol{\psi})_i = \sum_{j(i)}\left(\frac{1}{2}(\psi_i + \psi_{j(i)}) + \frac{L_{ij(i)}}{8}\big(\mathbf{h}^a_{ij(i)}\nabla_0^{(0.25,0.75)}\psi\big|_i - \mathbf{h}^b_{ij(i)}\nabla_0^{(0.25,0.75)}\psi\big|_{j(i)}\big)\right)\omega^\eta_{ij(i)}, \tag{5}$$

where $\gamma^\eta_{ij(i)} = (n^{\eta\,(1)}_{ij(i)}\,\delta l^{(1)}_{ij(i)} + n^{\eta\,(2)}_{ij(i)}\,\delta l^{(2)}_{ij(i)})/S(\Omega_i)$, $\omega^\eta_{ij(i)} = (\tau^{\eta\,(1)}_{ij(i)}\,\delta l^{(1)}_{ij(i)} + \tau^{\eta\,(2)}_{ij(i)}\,\delta l^{(2)}_{ij(i)})/S(\Omega_i)$, $\nabla_0^{(\beta_1,\beta_2)}\psi\big|_i = \sum_{ij(i)}(\beta_1\psi_i + \beta_2\psi_{j(i)})\boldsymbol{\gamma}_{ij(i)}$, $\mathbf{n}^{(k)}_{ij(i)}$, $\boldsymbol{\tau}^{(k)}_{ij(i)}$, $(k = 1, 2)$ are the vectors normal and tangential to the segment of the boundary crossing the edge connecting points i and j(i), $\delta l^{(k)}_{ij(i)}$, $(k = 1, 2)$ are the lengths of the segments of the boundary, and $S(\Omega_i)$ is the measure of the control volume Ω_i (see Fig. 2).

The time integration of (2) can be performed with different Ordinary Differential Equations (ODE) solvers depending on the time step used in the calculation. In the initial stage system (2) was integrated using the standard 4-th order Runge–Kutta method with the time step selected to assure that the Courant number was limited by 1. The "l norms", mass conservation error and the normalized indicators of the minimum and maximum values for $h^\star$ for tests 1 and 2 (described in [2]) performed on a geodesic mesh with 40962 nodes are shown in the following table:

	l_1	l_2	l_∞	$\mathcal{M}$	$f_{\min}$	$f_{\max}$
test 1 ($\alpha = \pi/2$)	2.83×10^{-4}	9.25×10^{-4}	7.50×10^{-3}	0.0	-0.01	0.98
test 2 ($\alpha = 0$)	4.62×10^{-5}	6.68×10^{-5}	3.46×10^{-4}	0.0	-0.0002	1.00

REFERENCES

[1] Pudykiewicz J., 2006: Numerical solution of the reaction–advection–diffusion equation on the sphere. *J. Comp. Phys.*, **213**, 358.

[2] Williamson D. L., J. B. Drake, J. J. Hack, R. Jakob, and P. N. Shwartzrauber, 1992: A Standard Test Set for Numerical Approximations to the Shallow Water Equations in Spherical Geometry. *J. Comp. Phys.*, **102**, 211.

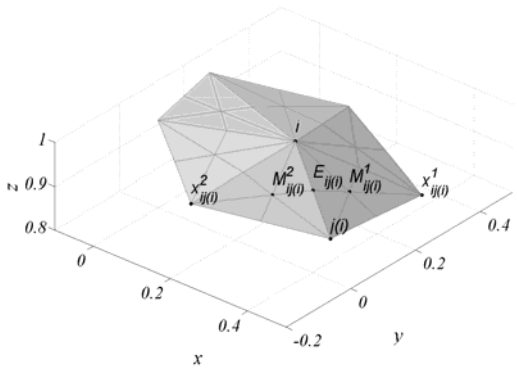

Fig. 1 Triangles used in the definition of the finite volumes on the sphere.

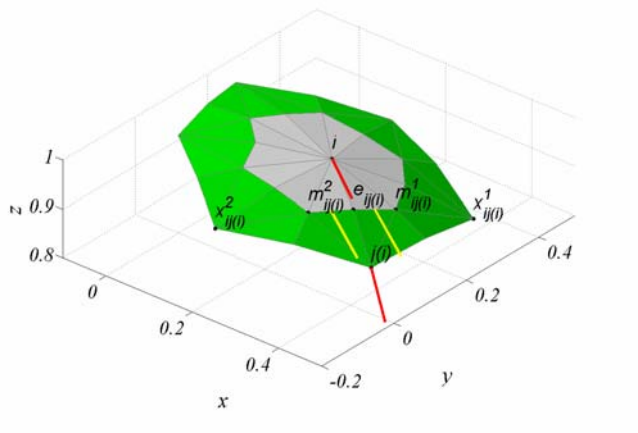

Fig. 2 The finite volume associated with a single node *i*.

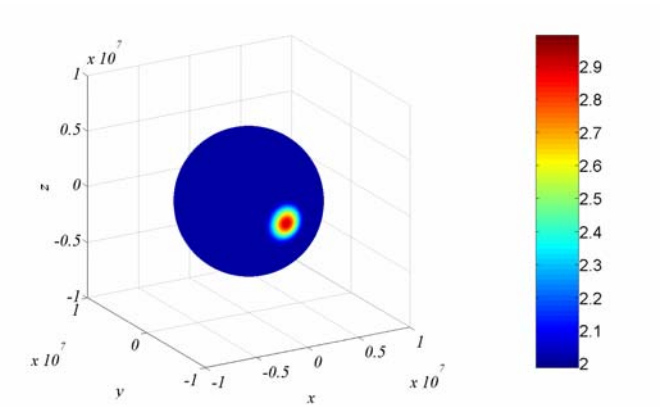

Fig. 3 Cosine hill after one rotation in flow crossing polar regions (test 1).

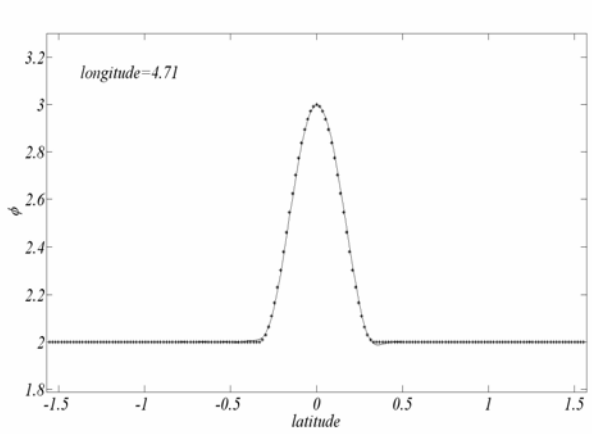

Fig. 4 Same as in Fig. 3 but the solution depicted by the solid line is that on the cross-section along the North-South plane (the analytical solution is represented by stars) .

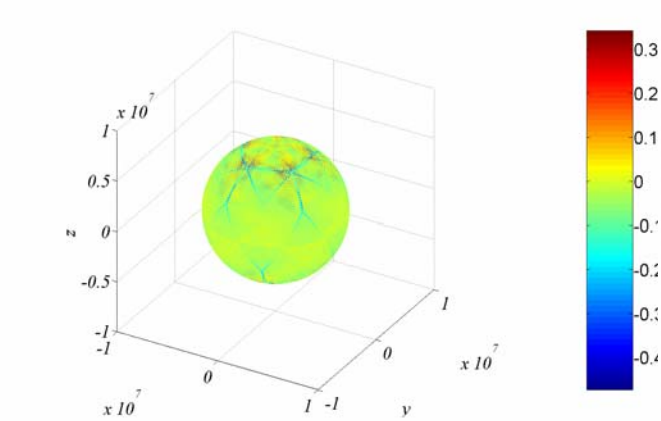

Fig. 5 The solution error for geopotential after 5 days for the global steady state nonlinear geostrophic flow (test 2).

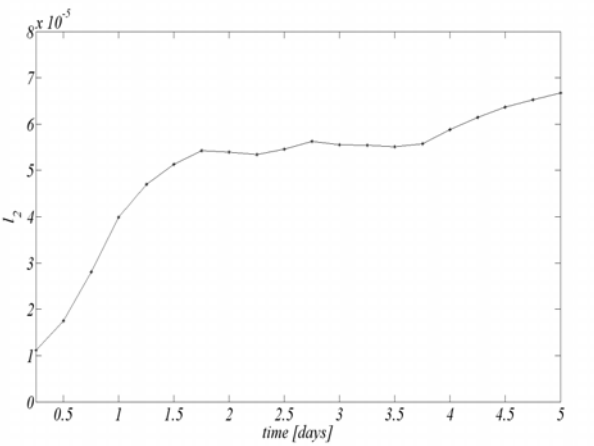

Fig. 6 The evolution of "l2" norm for the global steady state nonlinear geostrophic flow.

A three-dimensional conservative semi-Lagrangian scheme (SLICE-3D) for transport problems*

M. Zerroukat, N. Wood and A. Staniforth
Met Office, FitzRoy Road, Exeter EX1 3PB, U.K.

6th February 2006

Last year we reported on the development of an inherently conservative semi-Lagrangian (SLICE) scheme for two-dimensional passive transport in spherical geometry [1]. Since then, the reconstruction part of the scheme has been further developed by introducing the parabolic spline method (PSM), an optimal reconstruction having the minimum norm (or curvature) and best approximation properties [2]. Furthermore an improved grid and sub-grid scale monotonicity filter [2] has also been incorporated into the scheme. This filter is more selective and less damping in the smooth part of the solution than other filters.

A three-dimensional version of SLICE has now been developed in spherical geometry and tested on a variety of flows (see the example of figure 1). SLICE-3D does one sweep of a one-dimensional conservative remapping for each column in the vertical direction. This results in the transfer of mass contained between the original regular concentric spherical shells ($k = 1, ..., K$) to intermediate deformed concentric spherical shells ($k' = 1, ..., K$). This is followed by $(K - 1)$ applications of SLICE-2D around the $K - 1$ concentric deformed spherical annulii. Each application of SLICE-2D also makes multiple sweeps of the same one-dimensional remapping along physical distances around the deformed spherical annulii. It is also worth noting that no knowledge of the complex 3D geometrical details of the individual Lagrangian volumes is required or computed at any stage of the computation. This confers a significant efficiency advantage on the SLICE methodology over fully geometrical remapping algorithms. The resulting scheme makes the possibility of higher-dimensional remapping with high-order reconstructions, without a prohibitive computational cost, a reality.

References

[1] M. Zerroukat, N. Wood, A. Staniforth, SLICE-S: A Semi-Lagrangian Inherently Conserving and Efficient scheme for transport problems on the Sphere, Q. J. R. Meteorol. Soc. 130 (2004) 2649–2664.

[2] M. Zerroukat, N. Wood, A. Staniforth, The Parabolic Spline Method (PSM) for conservative transport problems, Int. J. Numer. Meth. Fluid (in press).

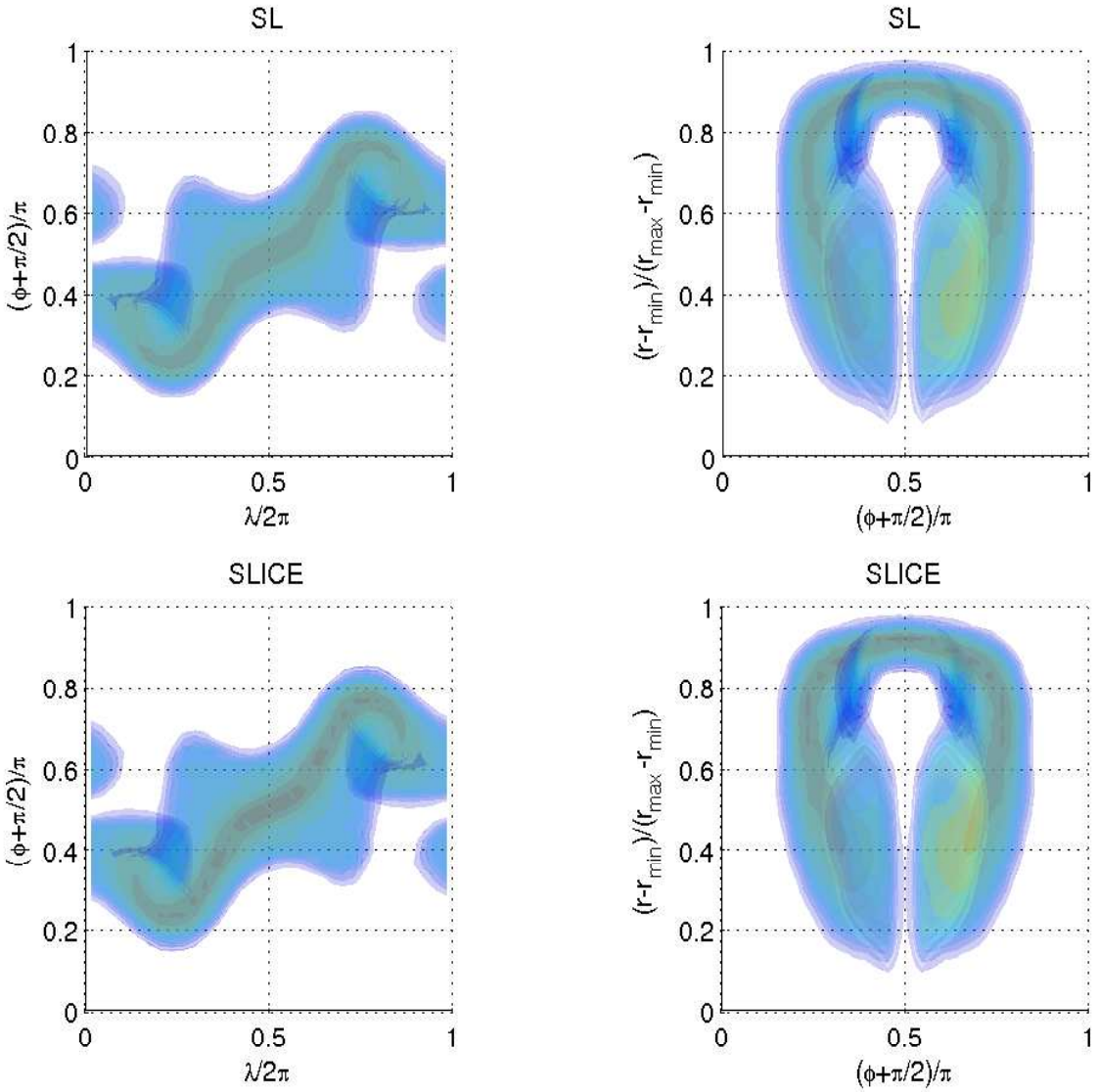

Figure 1: Comparison of results using the SLICE (bottom pair of plots) and standard tri-cubic interpolating Semi-Lagrangian (SL, top pair of plots) algorithms, in a spherical annulus lying between $r_{min} = 1$ and $r_{max} = 2$. A spherical distribution of mass, spanning approximately 1/3rd of the domain in each direction, is initially centred at the equator on the $\lambda = \pi$ meridian. It is then subjected to a flow field given by the superposition of stationary idealisations of a Rossby wave and a Hadley cell circulation. Two views of the solutions at $t = 1$, performed with timestep $\Delta t = 0.1$ and $32 \times 32x32$ control volumes(λ, ϕ, r), are displayed: the left and right pairs are (λ, ϕ) and (ϕ, r) views respectively.